



# Thiazolo[5,4- f ]quinoxalines, Oxazolo[5,4- f ]quinoxalines and Pyrazino[ b,e ]isatins: Synthesis from 6-Aminoquinoxalines and Properties

Frédéric Lassagne, Joshua M. Sims, William Erb, Olivier Mongin, Nicolas Richy, Nour El Osmani, Ziad Fajloun, Laurent Picot, Valérie Thiéry, Thomas Robert, et al.

## ► To cite this version:

Frédéric Lassagne, Joshua M. Sims, William Erb, Olivier Mongin, Nicolas Richy, et al.. Thiazolo[5,4- f ]quinoxalines, Oxazolo[5,4- f ]quinoxalines and Pyrazino[ b,e ]isatins: Synthesis from 6-Aminoquinoxalines and Properties. European Journal of Organic Chemistry, 2021, 2021 (19), pp.2756-2763. 10.1002/ejoc.202100362 . hal-03269555

**HAL Id: hal-03269555**

**<https://univ-rennes.hal.science/hal-03269555>**

Submitted on 30 Jun 2021

**HAL** is a multi-disciplinary open access archive for the deposit and dissemination of scientific research documents, whether they are published or not. The documents may come from teaching and research institutions in France or abroad, or from public or private research centers.

L'archive ouverte pluridisciplinaire **HAL**, est destinée au dépôt et à la diffusion de documents scientifiques de niveau recherche, publiés ou non, émanant des établissements d'enseignement et de recherche français ou étrangers, des laboratoires publics ou privés.

# Thiazolo[5,4-*f*]quinoxalines, oxazolo[5,4-*f*]quinoxalines and pyrazino[*b,e*]isatins: synthesis from 6-aminoquinoxalines and properties

Frédéric Lassagne,<sup>\*,[a]</sup> Joshua M. Sims,<sup>[a,b]</sup> William Erb,<sup>[a]</sup> Olivier Mongin,<sup>[a]</sup> Nicolas Richy,<sup>[a]</sup> Nour El Osmani,<sup>[c]</sup> Ziad Fajloun,<sup>\*,[c,d]</sup> Laurent Picot,<sup>\*,[e]</sup> Valérie Thiéry,<sup>[e]</sup> Thomas Robert,<sup>[f,g]</sup> Stéphane Bach,<sup>\*,[f,g,h]</sup> Vincent Dorcet,<sup>[a]</sup> Thierry Roisnel<sup>[a]</sup> and Florence Mongin<sup>\*,[a]</sup>

- [a] F. Lassagne, J. M. Sims, Dr. W. Erb, Dr. O. Mongin, N. Richy, Dr. V. Dorcet, Dr. T. Roisnel, Prof. F. Mongin  
Univ Rennes, CNRS, ISCR (Institut des Sciences Chimiques de Rennes) - UMR 6226, F-35000 Rennes, France  
E-mails: frederic.lassagne@univ-rennes1.fr, florence.mongin@univ-rennes1.fr
- [b] J. M. Sims  
Univ. Lyon, ENS de Lyon, CNRS UMR 5182, Université Claude Bernard Lyon 1, Laboratoire de Chimie, F-69342 Lyon, France
- [c] N. El Osmani  
Laboratory of Applied Biotechnology (LBA3B), Azm Center for Research in Biotechnology and its Applications, EDST, Lebanese University, 1300 Tripoli, Lebanon
- [d] Prof. Z. Fajloun  
Faculty of Sciences 3, Lebanese University, Campus Michel Slayman 1352 Ras Maska - Tripoli, Lebanon  
E-mail: ziad.fajloun@ul.edu.lb
- [e] Dr. L. Picot, Prof. V. Thiéry  
La Rochelle Université, Laboratoire Littoral Environnement et Sociétés, UMRi CNRS 7266, 17042 La Rochelle, France  
E-mail: laurent.picot@univ-lr.fr
- [f] T. Robert, Dr. S. Bach  
Sorbonne Université, CNRS, FR2424, Plateforme de criblage KISSf (Kinase Inhibitor Specialized Screening facility), Station Biologique de Roscoff, Place Georges Teissier, 29682 Roscoff, France  
E-mail: bach@sb-roscoff.fr
- [g] T. Robert, Dr. S. Bach  
Sorbonne Université, CNRS, UMR 8227, Integrative Biology of Marine Models, Station Biologique de Roscoff, CS 90074, 29688 Roscoff Cedex, France
- [h] Dr. S. Bach  
Centre of Excellence for Pharmaceutical Sciences, North-West University, Private Bag X6001, Potchefstroom 2520, South Africa

Supporting information for this article is given via a link at the end of the document.

**Abstract:** The regioselective iodination of different 2-mono-, 3-mono- and 2,3-disubstituted 6-aminoquinoxalines, which takes place at their 5-position, was rationalized on the basis of Hückel theory calculations. Oxazolo- and thiazolo[5,4-*f*]quinoxaline analogues of reported disease-related protein kinases inhibitors were synthesized from the obtained 6-amino-5-iodoquinoxalines by using as key steps copper-catalyzed azole ring formation. Pyrazino[*b,e*]isatins were for the first time obtained from the same substrates by recourse to Sonogashira coupling, alkyne hydration and oxidative cyclization. The absorption and emission properties of the most promising compounds were recorded. In addition, most of the synthesized polycycles were evaluated as protein kinase inhibitors and for their antiproliferative activity towards cancer cells.

## Introduction

Oxazolo[5,4-*f*]quinoxalines, thiazolo[5,4-*f*]quinoxalines and pyrazino[*b,e*]isatins (Figure 1, top) share similar structures in which a pyrazine ring is fused to a (hetero)aromatic (benzoxazole,<sup>1</sup> benzothiazole<sup>2</sup> or isatin,<sup>3</sup> respectively) of biological interest. These compounds can also be seen as a quinoxaline ring fused to a five-membered heterocycle (oxazole,<sup>4</sup> thiazole<sup>4</sup> or 2,3-pyrrolidinedione,<sup>5</sup> respectively) found in numerous bioactive molecules. However, in spite of the potential of these structures in fields such as medicinal chemistry and materials, very few results have been reported on

the topic. Pyrazino[*b,e*]isatins have, to our knowledge, never been prepared.

While a few thiazolo[5,4-*f*]quinoxalines have been claimed in patents,<sup>6</sup> the first oxazolo[5,4-*f*]quinoxalines were prepared by our group in 2020,<sup>7</sup> and notably the 8-piperidino-2-(3-pyridyl) **FI-290** and the 2-(3-pyridyl)-8-thiomorpholino **CD-07** derivatives identified as potent inhibitors of glycogen-synthase kinase 3 (GSK3)<sup>8</sup> with respective IC<sub>50</sub> values of about 5 and 11 nM on the isoform GSK3α<sup>9</sup> (Figure 1, bottom).<sup>7</sup>

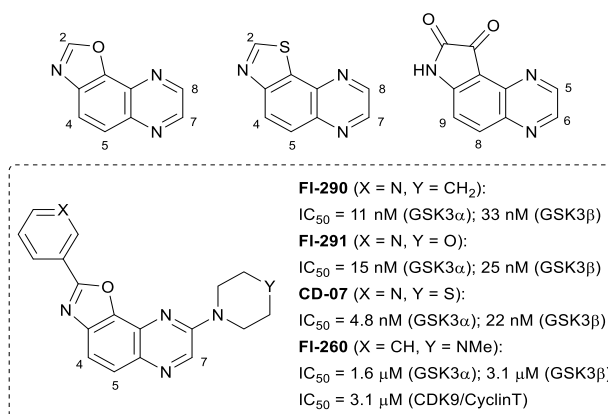


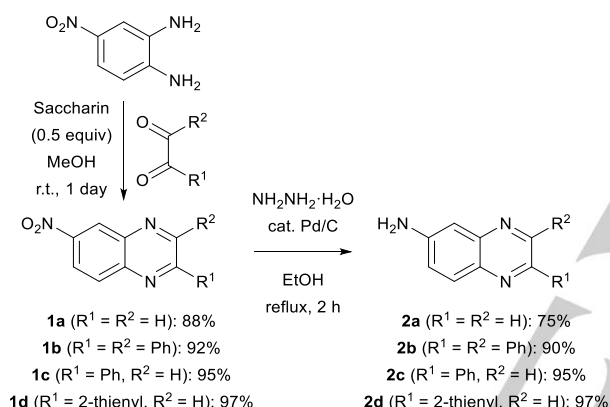
**Figure 1.** Top: Structures of oxazolo[5,4-*f*]quinoxaline (left), thiazolo[5,4-*f*]quinoxaline (middle) and pyrazino[*b,e*]isatin (right). Bottom: Recently discovered kinase inhibitors based on the oxazolo[5,4-*f*]quinoxaline skeleton.

Encouraged by these promising results, our goal in the present paper is to show that 6-amino-5-iodoquinoxalines can be used as common substrates to access these three families, to evaluate the photochemical properties of these compounds and to screen their biological activities.

## Results and Discussion

### Synthesis

We previously showed that 2- and 3-chloro-6-aminoquinoxalines could be regioselectively iodinated at C5-position by using iodine (2.5 equiv) and sodium hydrogenocarbonate (2.5 equiv) in a 4:1 dioxane-water mixture at room temperature.<sup>7</sup> As part of our ongoing research, we were eager to see if this interesting result could be extended to various 2-mono-, 3-mono- and 2,3-disubstituted substrates easily synthesized from 4-nitrophenylenediamine and various 1,2-dicarbonyl compounds under mild conditions (Scheme 1).<sup>10</sup>



**Scheme 1.** Regioselective synthesis of various 2-mono-, 3-mono- and 2,3-disubstituted 6-aminoquinoxalines **2**.

In order to firstly rationalize the regioselective iodination at C5 of 6-aminoquinoxalines and evaluate its scope with various substituents at C2 or/and C3, we used the HuLiS calculator<sup>11</sup> to get both the amplitudes of the highest occupied molecular orbital (HOMO) coefficients (Table 1) and the charges (Table 2) on the C atoms of various substituted 6-aminoquinoxalines series **2** and of quinoline analogues of **2a**.

The Hückel theory calculations<sup>12</sup> were inspired by a study of Begunov and co-workers in which the authors attributed the high regioselectivity in aromatic electrophilic substitution ( $S_{\text{E}}\text{Ar}$ ) of condensed imidazole derivatives to orbital control.<sup>13</sup> In our case, according to Fukui's concept (reaction of a compound with an electrophile at its carbon with the highest HOMO coefficient),<sup>14</sup> the reaction centre of the  $S_{\text{E}}\text{Ar}$  first step is the C5 atom, whatever of the nature of the substituents (when present) at C2 or/and C3 (Table 1). However, that the iodination is under orbital control cannot be inferred from these calculations. Indeed, by considering the charges on the different C atoms, the same result can be deduced, with the highest negative charge always localized at C5 (Table 2). Experimentally, all the performed reactions took place at C5 as expected, and proceeded in high yields ranging from 75 to 93% (Table 3; Figure 2).

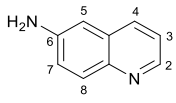
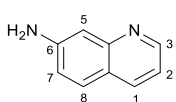
**Table 1.** HOMO orbital coefficients on the different C(H) atoms of the substituted 6-aminoquinoxalines **2**, and the 6- and 7-aminoquinolines.<sup>[a]</sup>

Entry	<b>2</b> (R <sup>1</sup> , R <sup>2</sup> )	C2	C3	C5	C7	C8
1	<b>2a</b> (H, H)	0.29	0.00	<b>0.54</b>	0.07	-0.32
2	<b>2b</b> (Ph, Ph)	-	-	<b>-0.38</b>	-0.15	0.26
3	<b>2c</b> (Ph, H)	-	-0.09	<b>-0.44</b>	-0.10	0.29
4	<b>2d</b> (2-thienyl, H)	-	-0.17	<b>-0.26</b>	-0.11	0.23
5	<b>2e</b> (Cl, H)	-	0.07	<b>0.49</b>	0.10	-0.31
6	<b>2f</b> (H, Cl)	-0.29	-	<b>-0.55</b>	-0.07	0.32
7	<b>2g</b> (H, Ph)	0.29	-	<b>-0.55</b>	-0.07	0.32
8	<b>2h</b> (OMe, OMe)	-	-	<b>0.43</b>	0.14	-0.29
9	<b>2i</b> (Cl, Cl)	-	-	<b>0.47</b>	0.12	-0.30
10	<b>2j</b> (Me, H)	-	0.06	<b>0.50</b>	0.09	-0.32
11	<b>2k</b> (H, Me)	-0.29	-	<b>-0.54</b>	-0.07	0.32
12	<b>2l</b> (NO <sub>2</sub> , H)	-	-0.28	<b>-0.55</b>	-0.06	0.32
13	<b>2m</b> (H, NO <sub>2</sub> )	-0.29	-	<b>-0.54</b>	-0.07	0.32
14		0.25	-0.12	C4: -0.32 C5: <b>0.52</b>	0.04	-0.34
15		C1: -0.22 C2: -0.34	0.02	<b>-0.55</b>	0.00	0.34

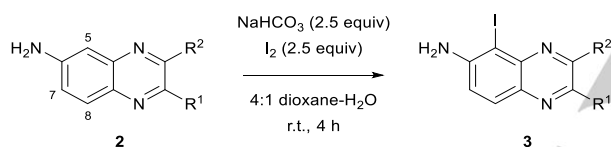
[a] For representations of the amplitudes and complete results of the calculations, see Supporting information. Because we used a numbering with the amino group fixed at the 6-position for all calculated substrates, the numbering for 7-aminoquinoline is not consistent with its name.

**Table 2.** Charges on the different C(H) atoms of the substituted 6-aminoquinoxalines **2**, and the 6- and 7-aminoquinolines.

Entry	<b>2</b> (R <sup>1</sup> , R <sup>2</sup> )	C2	C3	C5	C7	C8
1	<b>2a</b> (H, H)	0.08	0.10	<b>-0.09</b>	-0.02	0.00
2	<b>2b</b> (Ph, Ph)	-	-	<b>-0.10</b>	-0.03	0.00
3	<b>2c</b> (Ph, H)	-	0.11	<b>-0.09</b>	-0.02	0.00
4	<b>2d</b> (2-thienyl, H)	-	0.10	<b>-0.09</b>	-0.02	0.00
5	<b>2e</b> (Cl, H)	-	0.08	<b>-0.09</b>	-0.02	0.00
6	<b>2f</b> (H, Cl)	0.06	-	<b>-0.10</b>	-0.03	0.01

7	<b>2g</b> (H, Ph)	0.09	-	<b>-0.10</b>	-0.03	0.00
8	<b>2h</b> (OMe, OMe)	-	-	<b>-0.10</b>	-0.03	0.00
9	<b>2i</b> (Cl, Cl)	-	-	<b>-0.10</b>	-0.03	0.00
10	<b>2j</b> (Me, H)	-	0.08	<b>-0.09</b>	-0.02	0.00
11	<b>2k</b> (H, Me)	0.06	-	<b>-0.10</b>	-0.03	0.01
12	<b>2l</b> (NO <sub>2</sub> , H)	-	0.12	<b>-0.09</b>	-0.02	0.01
13	<b>2m</b> (H, NO <sub>2</sub> )	0.10	-	<b>-0.09</b>	-0.01	0.00
14		0.09	-0.01	C4: 0.05 C5: -0.08	-0.02	-0.01
15		C1: 0.07 C2: -0.02	0.10	<b>-0.10</b>	-0.04	0.02

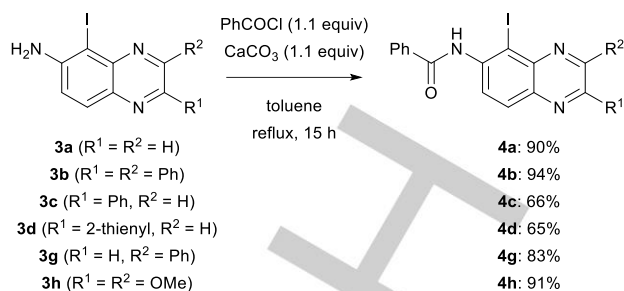
**Table 3.** Regioselective iodination of the different 2-mono-, 3-mono- and 2,3-disubstituted 6-aminoquinolines **2**.



Entry	<b>2</b> (R <sup>1</sup> , R <sup>2</sup> )	Product <b>3</b>	Yield (%) <sup>[a]</sup>
1	<b>2a</b> (H, H)	<b>3a</b>	83
2	<b>2b</b> (Ph, Ph)	<b>3b</b>	93
3	<b>2c</b> (Ph, H)	<b>3c</b>	93
4	<b>2d</b> (2-thienyl, H)	<b>3d</b>	85
5 <sup>[b]</sup>	<b>2e</b> (Cl, H)	<b>3e</b>	88
6 <sup>[b]</sup>	<b>2f</b> (H, Cl)	<b>3f</b>	88
7	<b>2g</b> (H, Ph)	<b>3g</b>	75
8	<b>2h</b> (OMe, OMe)	<b>3h</b>	86
9	<b>2i</b> (Cl, Cl)	<b>3i</b>	83

[a] After purification (see experimental part). [b] Results previously obtained.<sup>7</sup>

In order to progress towards the new oxazolo[5,4-*f*]quinolines **5a-d,g,h**, the 6-amino-5-iodoquinolines **3a-d,g,h** were *N*-benzoylated (Scheme 2), and the obtained carboxamides **4a-d,g,h** were cyclized to the corresponding oxazoles as previously reported<sup>7</sup> (Scheme 3).



**Scheme 2.** Benzoylation of the different 6-amino-5-iodoquinolines **3**.

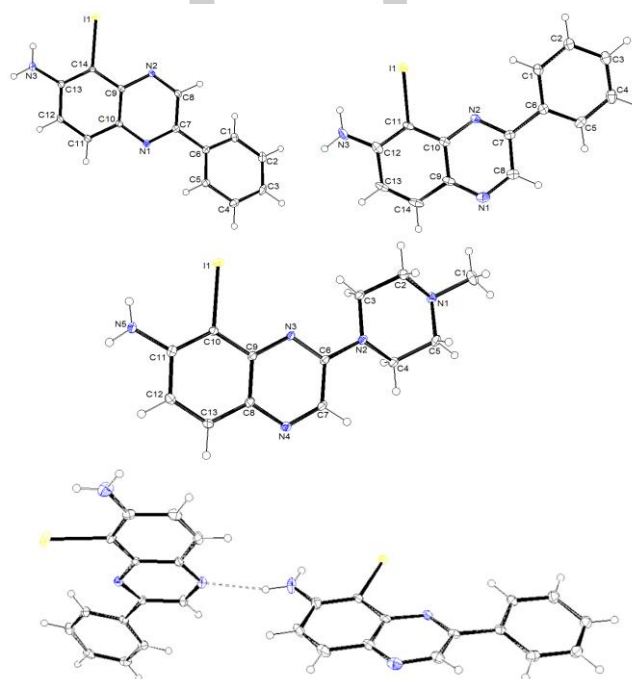
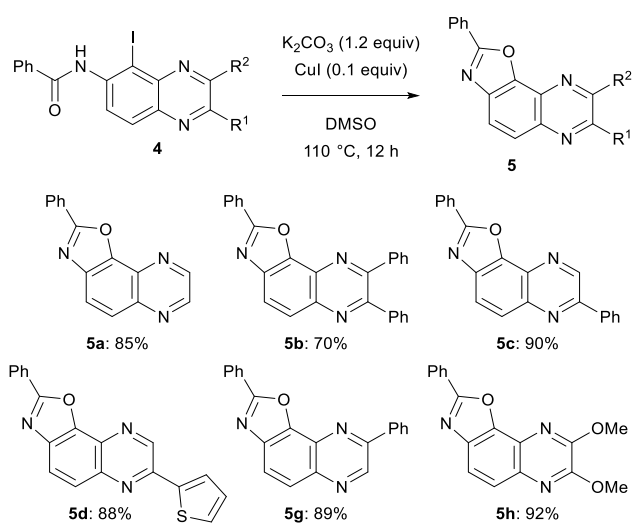
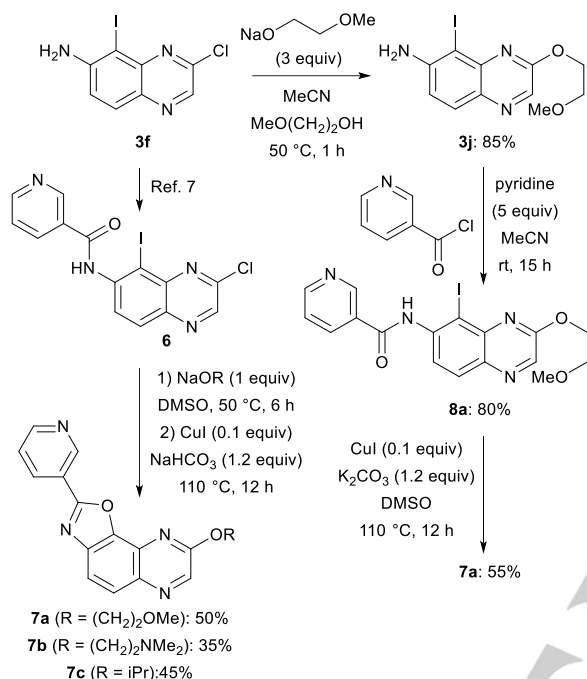


**Figure 2.** ORTEP diagrams (thermal ellipsoids shown at the 30% probability level) of the compounds **3c** (top left), **3g** (top right) and **3k** (middle, see Scheme 5), and H-bond (2.169 Å) in **3g** (bottom).



**Scheme 3.** Cyclization of compounds **4** to oxazolo[5,4-*f*]quinolines.

The synthesis of the oxazolo[5,4-*f*]quinoxalines **7a-c**, which are C8-alkoxy analogues of the GSK3 kinase inhibitors **FI-290** and **CD-07**, was also achieved from 6-amino-3-chloro-5-iodoquinoxaline (**3f**), either by a 'substitution of chlorine-arylation of amine-cyclization to oxazole' sequence (Scheme 4, top and right), or changing the step order with amine arylation followed by *one pot* chlorine substitution/oxazole ring formation (Scheme 4, left).

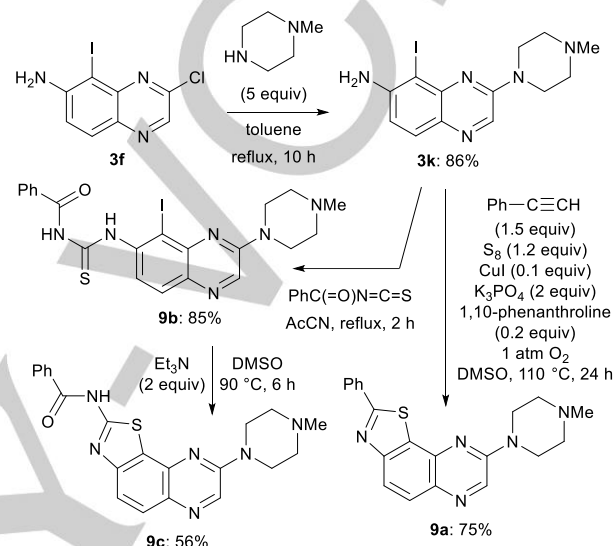


**Scheme 4.** Synthesis of alkoxy analogues of the GSK3 kinases inhibitors **FI-290** and **CD-07**.<sup>7</sup>

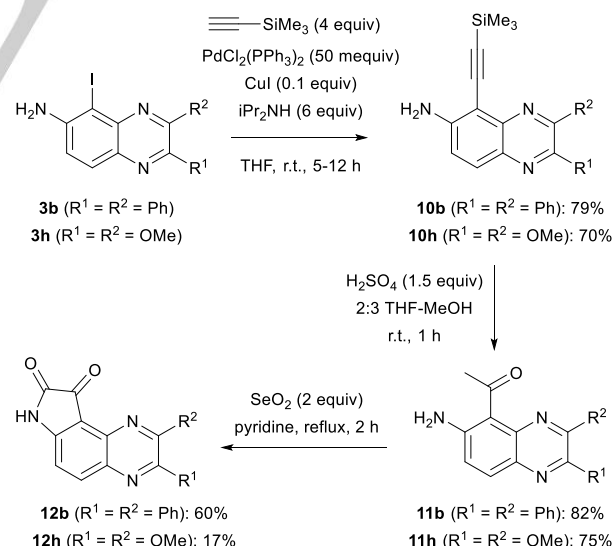
Very few thiazolo[5,4-*f*]quinoxalines have been obtained up to now by following lengthy syntheses.<sup>6</sup> We planned to investigate if this skeleton could be reached from 6-amino-5-iodoquinoxalines, and targeted the synthesis of the thiazolo[5,4-*f*]quinoxaline **9a**. The latter is a sulfur analogue of 8-(*N'*-methylpiperazino)-2-phenylthiazolo[5,4-*f*]quinoxaline (**FI-260**), an inhibitor of the disease-related protein kinases CDK9/CyclinT (cyclin-dependent kinase 9; IC<sub>50</sub> = 3.1 μM), GSK3α (IC<sub>50</sub> = 1.6 μM) and GSK3β (IC<sub>50</sub> = 3.1 μM). Inspired by the recent study of Wu and Jiang who used 2-iodoanilines, elemental sulfur (1.2 equiv) and terminal alkynes (1.5 equiv) in the presence of tripotassium phosphate (2 equiv) copper(I) iodide (0.1 equiv), 1,10-phenanthroline (0.2 equiv) under oxygen (1 atm) to prepare benzothiazole derivatives in dimethylsulfoxide (DMSO) at 110 °C,<sup>15</sup> the reaction of the 6-amino-5-iodoquinoxaline **3k** (coming from **3f**) with phenylacetylene under similar reaction conditions led to the expected product **9a** in 75% yield without further optimization (Scheme 5, top and right).

To progress towards thiazolo[5,4-*f*]quinoxalines having an additional substituent at C2, we were interested by the methodology reported by Verma and co-workers. Indeed, these authors showed in 2019 the possible synthesis of 2-(arylamino)benzothiazoles from 2-iodoanilines and aroyl isothiocyanate at 90 °C in water containing triethylamine (2

equiv).<sup>16</sup> In our case, we first prepared the 6-(*N'*-benzoyl)thioureido-5-iodoquinoxaline **9b** from **3k**, by reaction with benzoyl isothiocyanate at the reflux of acetonitrile. The cyclization of **9b**, which is less soluble than **3k**, to the 2-(benzoylamino)thiazolo[5,4-*f*]quinoxaline **9c** had to be performed at 90 °C in DMSO containing triethylamine (2 equiv) to reach a 56% yield. Thus, the original thiazolo[5,4-*f*]quinoxalines **9a** and **9c** were synthesized from 6-amino-3-chloro-5-iodoquinoxaline (**3f**) in respectively two and three steps and overall yields of 64.5 and 41% (Scheme 5, top and left).



**Scheme 5.** Synthesis of the thiazolo[5,4-*f*]quinoxalines **9a** (sulfur analogue of the kinase inhibitor **FI-260**) and **9c** from **3f**.



**Scheme 6.** Towards pyrazino-fused isatins from **3**.

As pyrazino[*b,e*]isatins have, to our knowledge, never been synthesized before, we were interested in the development of an approach towards these compounds. By starting from the 6-amino-5-iodoquinoxalines **3b** and **3h**, the required two-carbon



chain was introduced by Sonogashira coupling<sup>17</sup> with trimethylsilylacetylene under conditions reported by Mukai and co-workers.<sup>18</sup> Thus, in the presence of diisopropylamine, catalytic palladium(II) chloride bis(triphenylphosphine) and copper(I) iodide in tetrahydrofuran (THF) at room temperature, the reactions afforded **10b** and **10h** in correct yields (Scheme 6, top). The alkynes were next hydrated by using sulfuric acid in a mixture of solvents to provide the 5-acetyl-6-amino derivatives **11b** and **11h** in 82 and 75% yield, respectively (Scheme 6, right). Oxidative cyclization was finally applied by using selenium oxide in refluxing pyridine<sup>19</sup> to furnish the pyrazino-fused isatins **12b** and **12h** in 60 and 17% yield, respectively (Scheme 6, bottom).

### Photophysical properties

A preliminary study of the photophysical properties of selected compounds has been performed in order to identify potential fluorescent candidates combining protein kinase inhibition and fluorescence imaging or sensing properties. Such kind of compounds would be highly desirable tools to perform imaging studies of *in vitro* and/or *in vivo* protein kinase inhibition.<sup>20</sup> The UV-visible absorption and emission properties of **5d**, **5g** and **FI-290** were investigated in acetonitrile, and the results are gathered in Table 4.

**Table 4.** Absorption and emission properties of **5d**, **5g** and **FI-290** in CH<sub>3</sub>CN.

Compound	$\lambda_{\text{abs}}^a$ (nm)	$\epsilon_{\text{max}}^b$ (M <sup>-1</sup> cm <sup>-1</sup> )	$\lambda_{\text{em}}^c$ (nm)	$\Phi_F^d$
<b>5d</b>	312, 377	33300	431	0.09
<b>5g</b>	298, 351	38700	419	0.03
<b>FI-290</b>	300, 385	31400	455	0.08

[a] Absorption maxima. [b] Molar extinction coefficient at absorption maximum. [c] Emission maximum. [d] Fluorescence quantum yield using as a standard quinine bisulfate in 0.5 M H<sub>2</sub>SO<sub>4</sub>, upon excitation at lowest energy absorption maximum.

The three oxazoloquinoxalines **5d**, **5g** and **FI-290** exhibit two main absorption bands in the near UV, one of higher energy with a maximum near 300 nm and a large molar extinction coefficient ( $> 30000 \text{ M}^{-1} \text{ cm}^{-1}$ ), and the other one of lower energy with a maximum between 350 and 400 nm and lower absorptivity (Figure 3). These compounds are fluorescent and their emission band is situated in the violet-blue part of the visible. Compound **5d**, bearing two phenyl groups, is the less emissive, with a fluorescence quantum of 3%. Replacement of these phenyl groups with an electron-donating piperidiny group at the 8-position of the oxazoloquinoxaline and an electron-withdrawing pyridyl group on the other side leads to an increase of the quantum yield of **FI-290** up to 8%. A slightly higher fluorescence efficiency (9%) is obtained with **5g**, substituted with an electron-rich thienyl ring at the 7-position of the oxazoloquinoxaline. Moreover, the absorption and emission bands of **5d** and **FI-290** are red-shifted in comparison with **5g**, presumably in relation with an intramolecular charge transfer (ICT) process.

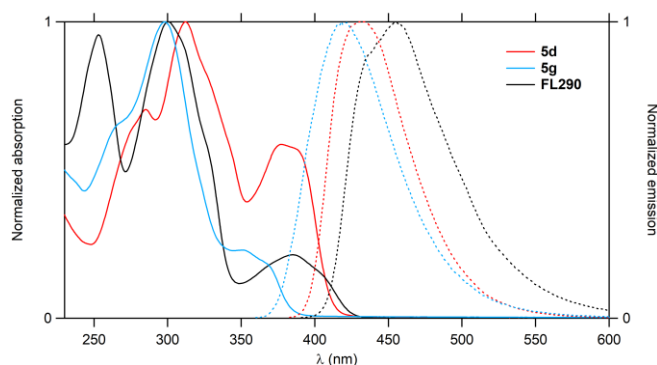


**Figure 3.** Absorption (solid line) and emission (dotted line) spectra of **5d**, **5g** and **FI-290** in acetonitrile.

### Bioactivity

Most of the synthesized compounds were evaluated in biological assays, first by looking at their antioxidant properties. As shown in Table 5, while the *in vitro* antioxidant activity of the derivatives does not exceed 60% of the DPPH radical scavenger activity (RSA), **5h** (64%) and above all **8a** (88%) can be considered as potent antioxidant compounds.

**Table 5.** Antioxidant activity (at  $t = 30$  min) of some of the synthesized compounds.

Compound	RSA (%) <sup>[a]</sup>	Compound	RSA (%) <sup>[a]</sup>
<b>5a</b>	57	<b>5h</b>	64
<b>5b</b>	35	<b>FI-290</b>	62
<b>5c</b>	56	<b>7a</b>	56
<b>5d</b>	31	<b>7c</b>	56
<b>5g</b>	49	<b>8a</b>	88

[a] 100  $\mu\text{g}$  tested at a concentration of 50  $\mu\text{g/mL}$  in DMSO at room temperature.

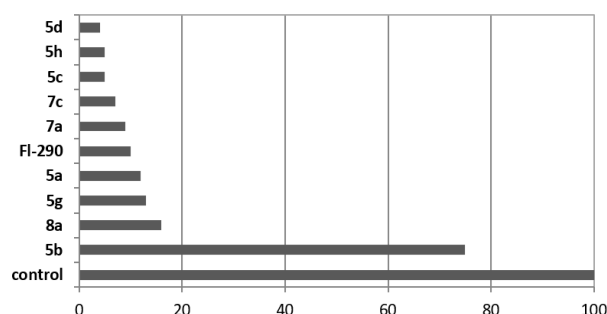


**Figure 4.** Cytotoxicity assay representing the antiproliferative effects (% viability) of some of the synthesized compounds on HCT116 (human colorectal) cancer cells. 100  $\mu\text{g}$  tested at a concentration of 1 g/L in DMSO at room temperature. Data are collected from  $n = 1$  experiment, and are expressed in % of maximal viability (DMSO control).

A study was also performed in order to investigate the antiproliferative activity of some of the prepared derivatives towards cancer cell lines. First, HCT116 (human colorectal) cancer cells were chosen to evaluate the cytotoxic potential of

the compounds **5a-d**, **5g,h**, **7a,c**, **8a** and **FI-290**. Pleasingly, except in the case of 2,7,8-triphenyloxazolo[5,4-*f*]quinoxaline (**5b**), a remarkable antiproliferative activity (>80%) was evidenced for all the tested compounds (Figure 4).

We also evaluated the antiproliferative activity of the compounds **5b,d,h**, **7a,b,c**, **9c**, **11b,h**, **12b,h**, **FI-290**, **FI-291** and **CD-07** against the A2058 melanoma cell line, considered as highly resistant to anticancer drugs. Molecules at  $10^{-5}$  M induced a growth inhibition at 72 h ranging from 0.3% to 66% (Figure 5). The original thiazolo[5,4-*f*]quinoxaline **9c** showed a promising antiproliferative activity against the selected melanoma cells.

Because they are often deregulated in diseases such as cancers and neurodegenerative disorders, protein kinases have become a major class of drug targets.<sup>21</sup> As part of our ongoing studies on the discovery of new protein kinase inhibitors,<sup>19,22</sup> most of the compounds here synthesized were tested<sup>7</sup> against several disease-related protein kinases: cyclin-dependent kinases 2 (CDK2/Cyclin A), 5 (CDK5/p25) and 9 (CDK9/Cyclin T), proto-oncogene kinase PIM1, CDC2-like kinase 1 (CLK1), dual specificity tyrosine phosphorylation regulated kinase 1A (DYRK1A), glycogen-synthase kinase-3 (GSK-3 isoforms  $\alpha/\beta$ ), casein kinase 1 (CK1 isoforms  $\delta/\epsilon$ ), mitotic kinase Haspin and vascular endothelial growth factor receptor 2 (VEGFR2).

As shown in Table 5, the compounds **7a-c** were found less efficient than the potent kinase inhibitors **FI-290**, **FI-291** and **CD-07**. When compared with **FI-260** which inhibits CDK9/CyclinT ( $IC_{50}$  = 3.1  $\mu$ M), GSK3 $\alpha$  ( $IC_{50}$  = 1.6  $\mu$ M) and GSK3 $\beta$  ( $IC_{50}$  = 3.1

$\mu$ M), its thiazolo[5,4-*f*]quinoxaline analogue **9a** is also less efficient. In addition, while a weak activity was noticed for most of the tested derivatives, compound **9c** was found active against CK1 at both 10  $\mu$ M and 1  $\mu$ M. Therefore, to clearly establish its potency, its  $IC_{50}$  values of inhibition against both CK1 $\epsilon$  (0.31  $\mu$ M) and CK1 $\delta/\epsilon$  (1.58  $\mu$ M) were determined, thus establishing **9c** as a potent CK1 kinase inhibitor.

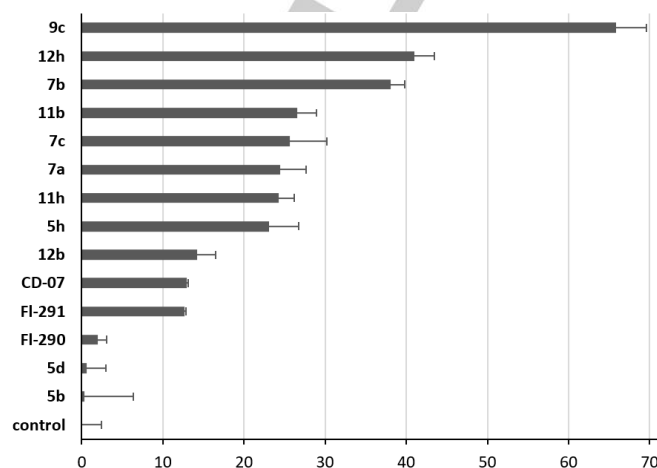


**Figure 5.** Antiproliferative activity (% growth inhibition) of compounds here synthesized at  $10^{-5}$  M after 72 h in 2000 A2058 human melanoma cells (DMSO control).

**Table 5.** Inhibitory activities of some of the synthesized compounds against a short panel of disease-related protein kinases. The table displays the remaining kinase activities detected after treatment with 10 and 1  $\mu$ M of the tested compounds. The values obtained after treatment with 1  $\mu$ M are given in brackets. Results are expressed in % of maximal activity, i.e. measured in the absence of inhibitor but with an equivalent dose of DMSO (solvent of the tested compounds). ATP concentration used in the kinase assays was 10  $\mu$ mol/L (values are means, n = 2). Kinases are from human origin unless specified: *Mm*, *Mus musculus*; *Rn*, *Rattus norvegicus*; *Ssc*, *Sus scrofa domestica*.

Compd.	CDK2/ CyclinA	CDK5/ p25	CDK9/ CyclinT	PIM1	<i>Mm</i> CLK1	<i>Rn</i> DYRK1A	GSK3 $\alpha$	GSK3 $\beta$	<i>Ssc</i> GSK3 $\alpha/\beta$	CK1 $\epsilon$	<i>Ssc</i> CK1 $\delta/\epsilon$	Haspin	VEGFR2
<b>5a</b>	[a]		67 (84)	92 (96)	[b]	[b]	83 (91)	91 (82)	84 ( $\geq 100$ )	93 (97)	[b]	[b]	[b]
<b>5b</b>	[a]	[a]	66 (96)	$\geq 100$ (99)	[b]	[b]	$\geq 100$ (94)	99 (93)	[a]	[a]	[b]	[b]	[b]
<b>5c</b>	90 ( $\geq 100$ )	[a]	53 (93)	96 (99)	[b]	[b]	[a]	98 (64)	[a]	[a]	[b]	[b]	[b]
<b>5d</b>	92 ( $\geq 100$ )	$\geq 100$ (93)	100 (78)	94 ( $\geq 100$ )	[b]	[b]	[a]	$\geq 100$ (73)	98 ( $\geq 100$ )	$\geq 100$ (97)	[b]	[b]	[b]
<b>5g</b>	$\geq 100$ (94)	[a]	87 (99)	97 (90)	[b]	[b]	94 (79)	94 (73)	85 (77)	[a]	[b]	[b]	[b]
<b>5h</b>	96 ( $\geq 100$ )	[a]	63 (71)	[a]	[b]	[b]	[a]	$\geq 100$ (79)	[a]	[a]	[b]	[b]	[b]
<b>7a</b>	[b]	[b]	61 (76)	39 (98)	[b]	<b>14 (31)</b>	<b>28 (45)</b>	34 (69)	[b]	[a]	[b]	33 (61)	[a]
<b>7b</b>	[b]	[b]	66 (68)	90 ( $\geq 100$ )	[b]	<b>15 (49)</b>	<b>32 (41)</b>	34 (64)	[b]	[a]	[b]	43 (60)	[a]
<b>7c</b>	[b]	[b]	92 (80)	44 (79)	[b]	<b>19 (43)</b>	26 (50)	38 (69)	[b]	75 ( $\geq 100$ )	[b]	18 (57)	72 ( $\geq 100$ )
<b>FI-290</b> <sup>7</sup>	[b]	58 (97)	<b>11 (40)</b>	13 ( $\geq 100$ )	[b]	<b>4 (21)</b>	<b>11 (13)</b>	<b>1 (5)</b>	[b]	83 (93)	[b]	21 (58)	[b]
<b>FI-291</b> <sup>7</sup>	[b]	66 (98)	<b>23 (43)</b>	<b>23 (43)</b>	[b]	<b>3 (11)</b>	<b>9 (9)</b>	<b>2 (2)</b>	[b]	65 (75)	[b]	<b>12 (23)</b>	[b]
<b>CD-07</b> <sup>7</sup>	[b]	53 (99)	4 (69)	18 ( $\geq 100$ )	[b]	<b>5 (19)</b>	<b>-1 (-3)</b>	<b>21 (14)</b>	[b]	44 (86)	[b]	8 (63)	[b]
<b>9a</b>	86 ( $\geq 100$ )	[a]	57 (64)	98 ( $\geq 100$ )	[b]	[b]	57 (99)	55 (99)	58 ( $\geq 100$ )	90 ( $\geq 100$ )	86 ( $\geq 100$ )	61 (69)	[b]
<b>FI-260</b> <sup>7</sup>	52 (98)	85 (81)	4 (61)	75 (89)	[b]	[b]	-7 (54)	12 (58)	14 (69)	40 (94)	[b]	[b]	[b]
<b>9c</b>	[a]	$\geq 100$ (91)	73 ( $\geq 100$ )	88 (91)	[b]	[b]	86 ( $\geq 100$ )	90 (99)	85 (92)	24 (67) <sup>[c]</sup>	<b>9 (39)</b> <sup>[d]</sup>	89 (90)	[b]
<b>11b</b>	99 (100)	[b]	$\geq 100$ (96)	42 (98)	89 ( $\geq 100$ )	[a]	[b]	[b]	$\geq 100$ (93)	[b]	[a]	[a]	[b]
<b>12b</b>	$\geq 100$ (96)	[b]	73 (98)	76 (98)	[a]	[a]	[b]	[b]	[a]	[b]	[a]	[a]	[b]
<b>12h</b>	93 (92)	[b]	89 (94)	[a]	[a]	[a]	[b]	[b]	[a]	[b]	[a]	95 ( $\geq 100$ )	[b]

[a]  $\geq 100$  ( $\geq 100$ ). [b] Not determined. [c]  $IC_{50}$  = 0.31  $\mu$ M. [d]  $IC_{50}$  = 1.58  $\mu$ M.

## Conclusion

In the present study, we have first rationalized the regioselective iodination at their 5-position of 2-mono-, 3-mono- and 2,3-disubstituted 6-aminoquinoxalines, and used the reaction to access original derivatives in which a pyrazine ring is fused to a benzoxazole, a benzothiazole and, for the first time, even an

isatin. It is worth noting that the Hückel theory calculations similarly predict a regioselective halogenation at the 5-position for 6-aminoquinoxaline,<sup>23</sup> and at the 8-position for 7-aminoquinoxaline.<sup>24</sup>

An early photophysical evaluation of some of the compounds was performed and their biological properties were finally investigated. By this way, we not only managed to access new GSK3 kinase inhibitors, but also identified a new CK1 kinase selective inhibitor, therefore establishing these original

heterocycle-fused quinoxalines as promising scaffolds for drug development.

## Experimental Section

General information, analyses of the compounds and NMR spectra are given in Supporting information.

**General procedure 1 for the cyclocondensation.**<sup>10</sup> To the required 1,2-dicarbonyl compound (10 mmol) in methanol (10 mL) were added saccharin (92 mg, 0.50 mmol) and 4-nitrophenylenediamine (10 mmol). The reaction mixture was stirred at room temperature for 24 h and poured onto water (10 mL). The solid was collected by filtration and dried under reduced pressure to afford the title product which was used in the next step without further purification.

**General procedure 2 for the reduction of the nitro compounds.**<sup>25</sup> To a stirred suspension of the nitro compound (10 mmol) in EtOH (25 mL) were added Pd/C (0.30 g) and hydrazine hydrate (5.0 mL). After 30 min, the reaction mixture was heated under reflux for 2 h. After cooling to room temperature, filtration over Celite® and rinsing with AcOEt, the solvents were evaporated under reduced pressure. The solid was dissolved in AcOEt and the organic phase washed with brine. Drying over Na<sub>2</sub>SO<sub>4</sub> and removal of the solvent under reduced pressure led to the expected product which was employed in the next step without purification.

**General procedure 3 for the iodination of the amino compounds.**<sup>7</sup> To a solution of the amine (17 mmol) in 4:1 dioxane-water (80 mL) at 0 °C were successively added NaHCO<sub>3</sub> (3.5 g, 42 mmol) and I<sub>2</sub> (11 g, 42 mmol). The solution was stirred at room temperature for 4 h and poured onto a saturated aqueous Na<sub>2</sub>S<sub>2</sub>O<sub>3</sub> solution (40 mL). The product was extracted with CH<sub>2</sub>Cl<sub>2</sub> (3 x 20 mL); the organic layer was washed with water (20 mL) and dried over Na<sub>2</sub>SO<sub>4</sub>. After evaporation of the solvent under reduced pressure, the iodide was purified as indicated in the product description (see an example below).

**6-Amino-5-iodoquinoxaline (3a).**<sup>26</sup> The general procedure 3 from 6-aminoquinoxaline (**2a**; 2.5 g) gave, after purification by chromatography over silica gel (eluent: CH<sub>2</sub>Cl<sub>2</sub>; R<sub>f</sub> = 0.59), **3a** in 83% yield (3.8 g) as a dark red solid: mp 180-182 °C; IR (ATR): 507, 861, 950, 1042, 1419, 1494, 1534, 1618, 3186, 3297, 3444 cm<sup>-1</sup>; <sup>1</sup>H NMR (CDCl<sub>3</sub>) δ 4.87 (br s, 2H, NH<sub>2</sub>), 7.26 (d, 1H, J = 9.0 Hz, H7), 7.85 (d, 1H, J = 9.0 Hz, H8), 8.54 (d, 1H, J = 1.9 Hz, H2), 8.75 (d, 1H, J = 1.9 Hz, H3); <sup>13</sup>C NMR (CDCl<sub>3</sub>) δ 83.0 (C, C5, C-I), 120.8 (CH, C7), 130.5 (CH, C8), 138.8 (C), 141.5 (CH, C2 or C3), 144.4 (C), 145.6 (CH, C2 or C3), 149.5 (C).

**General procedure 4 for the conversion of the amines into benzamides.**<sup>7</sup> To a suspension of the amine (2.0 mmol) and calcium carbonate (0.22 g, 2.2 mmol) in toluene (10 mL) was added benzoyl chloride (0.31 g, 2.2 mmol). The mixture was heated under reflux for 15 h. After filtration of the hot solution, the filtrate was concentrated under reduced pressure to give the expected product which was used in the next step without further purification.

**General procedure 5 for the cyclization of the iodinated amides.**<sup>7</sup> To a suspension of the iodinated amide (0.125 mmol) in dry DMSO (0.5 mL) under argon was added K<sub>2</sub>CO<sub>3</sub> (20 mg, 0.15 mmol) and CuI (2.4 mg, 12.5 μmol). The reaction mixture was heated at 110 °C for 12 h and cooled. The resulting dark mixture was poured onto a cold saturated aqueous NaHCO<sub>3</sub> solution (5 mL); the precipitate was filtered, washed with cold water and dissolved in CHCl<sub>3</sub>. The organic layer was dried over Na<sub>2</sub>SO<sub>4</sub> and the solvent was removed under reduced pressure. The product was purified as specified below.

**General procedure 6 for the conversion of 6-(3-pyridoylamino)-3-chloro-5-iodoquinoxaline (6) by nucleophilic substitution followed by cyclization.** To 6-(3-pyridoylamino)-3-chloro-5-iodoquinoxaline (**6**; 51 mg, 0.125 mmol) under argon were added anhydrous DMSO (0.5 mL) and the required sodium ethanolate (prepared by heating under argon the 2-substituted ethanol in the presence of 60% NaH (1 equiv) in dry toluene at 50 °C for 1 h before removal of the solvent, addition of dry Et<sub>2</sub>O and filtration; 0.15 mmol). The red reaction mixture was stirred at 50 °C for 6 h. CuI (2.6 mg, 12.5 μmol) was next added, followed by NaHCO<sub>3</sub> (13 mg, 0.15 mmol), and the reaction mixture was heated at 110 °C for 12 h. The reaction was monitored by TLC using CH<sub>2</sub>Cl<sub>2</sub>-MeOH 90:10 as eluent. When the reaction was finished, the solvent was removed under reduced pressure. The residue was dissolved in CHCl<sub>3</sub>, washed with brine. Drying over Na<sub>2</sub>SO<sub>4</sub> and removal of the solvent under reduced pressure led to the crude product which was purified by preparative TLC plate on silica gel (the eluent is given in the product description).

**General procedure 7 for the Sonogashira coupling.**<sup>18</sup> Anhydrous tetrahydrofuran (4 mL) was degassed 5 min with argon and introduced into a Schlenk tube containing the iodoquinoxaline (1.5 mmol). To the solution obtained after stirring, were added CuI (28.5 mg, 0.15 mmol) and PdCl<sub>2</sub>(PPh<sub>3</sub>)<sub>2</sub> (52.5 mg, 75 μmol). The mixture was stirred under argon for 5 min before addition of degassed anhydrous iPr<sub>2</sub>NH (1.3 mL, 9.6 mmol) and (trimethylsilyl)acetylene (0.80 mL, 5.7 mmol). After 5 h stirring at room temperature, the reaction mixture was partitioned between AcOEt and H<sub>2</sub>O. The organic layer was washed with brine and dried over Na<sub>2</sub>SO<sub>4</sub>. Removal of the solvent under reduced pressure led to the crude product which was purified by column chromatography over silica gel (eluent given in the product description).

**General procedure 8 for the conversion of 10 into 11.** A solution of **10** (0.20 g, 0.5 mmol) in tetrahydrofuran (2 mL) was added to a solution of H<sub>2</sub>SO<sub>4</sub> (83 μL, 1.5 mmol) in methanol (3 mL). The mixture was stirred for 1 h and evaporated. The residue was dissolved in AcOEt and washed with a saturated aqueous NaHCO<sub>3</sub> solution and then brine. The organic phase was dried over Na<sub>2</sub>SO<sub>4</sub>. Removal of the solvent under reduced pressure led to the crude product which was purified by column chromatography over silica gel (eluent given in the product description).

**General procedure 9 for the conversion of 11 into isatins.**<sup>19</sup> To the ketone (**11**; 0.50 mmol) in pyridine (1 mL) was added SeO<sub>2</sub> (115 mg, 1.0 mmol). The mixture was heated under reflux for 2 h. After cooling to room temperature, an aqueous 1 M solution of HCl (2 mL) was added before filtration and washing with H<sub>2</sub>O (2 x 5 mL). Drying under vacuum afforded the isatin.

**Cellular viability assay.** HCT116 cells were obtained from the American Type Culture Collection (ATCC). The cell line was cultured in DMEM (Gibco Dulbecco's Modified Eagle Medium, Sigma Aldrich) at 37 °C in a humidified atmosphere 5% CO<sub>2</sub> and 95% air. Media was amplified with 1% Penicillin Streptomycin (100 U·mL<sup>-1</sup>) and 10% heat-inactivated fetal bovine serum (FBS). The cellular viability assay was carried out by MTT (3-(4,5-dimethyl-2-thiazolyl)-2,5-diphenyltetrazolium bromide) test. MTT assay works on the mitochondria of the cell by the enzyme mitochondrial reductase.<sup>27</sup> It converts the yellow dye of MTT to purple formazan. Cells were seeded in 96 well plates at a density of 10<sup>4</sup>. At 70% confluency, the cells are ready to be treated. The treatment was for 24 h. After 24 h, the media was discarded. 100 μL of MTT solution was added to each well. The absorbance was measured by ELISA READER at 570 nm. The antiproliferative activity in A2058 melanoma cells (LGC Promochem, France) was evaluated as previously reported by our team.<sup>19</sup>

**Biological evaluation: protein kinase assays.** Kinase activities were assayed in 384-well plates using the ADP-Glo™ assay kit following the recommendations of the manufacturer (Promega, Madison, WI). The experimental conditions used to detect the enzymatic activity of each protein kinase tested in this study are reported.<sup>28</sup> Controls were



performed in appropriate dilutions of dimethyl sulfoxide (DMSO). IC<sub>50</sub> values were determined from the dose response curves using Prism-GraphPad (GraphPad Software, San Diego, CA, USA).

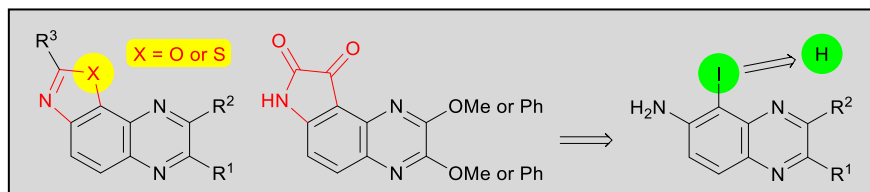
## Acknowledgements

We thank the "Comité d'Ille et Vilaine 35" de la Ligue Nationale Contre le Cancer, the Université de Rennes 1 and the Centre National de la Recherche Scientifique for supporting this research. We acknowledge the Fonds Européen de Développement Régional (FEDER; D8 VENTURE Bruker AXS diffractometer). V. T. and L. P. also thank the "Comité 17 de la Ligue Nationale Contre le Cancer for financial support. T. R. and S. B. thank IBI SA (French Infrastructures en Sciences du Vivant: Biologie, Santé et Agronomie), the Cancéropôle Grand Ouest ("Marines molecules, metabolism and cancer" network) and Biogenouest (Western France Life Science and Environment Core Facility Network) for supporting the KISSf screening facility (FR2424, CNRS and Sorbonne Université), Roscoff, France. We thank Dr. Pratyay Basak for his contribution to this study.

**Keywords:** quinoxaline • iodination • oxazole • regioselectivity • kinase inhibitor

- [1] C. S. Demmer, L. Bunch, *Eur. J. Med. Chem.* **2015**, *97*, 778-785.
- [2] Y.-J. Wu, *Top. Heterocycl. Chem.* **2012**, *29*, 307-328.
- [3] a) H. Guo, *Eur. J. Med. Chem.* **2019**, *164*, 678-688; b) P. A. Teixeira De Moraes Gomes, L. J. Pena, A. C. Lima Leite, *Mini-Rev. Med. Chem.* **2019**, *19*, 56-62.
- [4] a) D. Davyt, G. Serra, *Marine Drugs* **2010**, *8*, 2755-2780; b) Z. Jin, *Nat. Prod. Rep.* **2013**, *30*, 869-915.
- [5] E. M. Afsah, S. M. Abdelmageed, *J. Heterocycl. Chem.* **2020**, *57*, 3763-3783.
- [6] a) P. Jacobsen, F. E. Nielsen, T. Honore, J. Drejer, **1990**, EP348872; b) G. Liu, Q. Zhong, R. Liu, **2016**, CN105272978.
- [7] F. Lassagne, C. Duguépéroux, C. Roca, C. Perez, A. Martinez, B. Baratte, T. Robert, S. Ruchaud, S. Bach, W. Erb, T. Roisnel, F. Mongin, *Org. Biomol. Chem.* **2020**, *18*, 154-162.
- [8] A. Prasanth Saraswati, S. M. Ali Hussaini, N. Hari Krishna, B. Nagendra Babu, A. Kamal, *Eur. J. Med. Chem.* **2018**, *144*, 843-858.
- [9] O. Silva-García, R. Cortés-Vieyra, F. N. Mendoza-Ambrosio, G. Ramírez-Galicia, V. M. Baizabal-Aguirre, *Biomolecules* **2020**, *10*, 1683.
- [10] F. Lassagne, F. Chevallier, F. Mongin, *Synth. Commun.* **2014**, *44*, 141-149.
- [11] N. Goudard, Y. Carissan, D. Hagebaum-Reignier, S. Humbel, *HuLiS* 3.3.4; see: <http://ism2.univ-amu.fr/hulis>.
- [12] a) Y. Carissan, D. Hagebaum-Reignier, N. Goudard, S. Humbel, *J. Phys. Chem. A* **2008**, *112*, 13256-13262; b) Y. Carissan, D. Hagebaum-Reignier, N. Goudard, S. Humbel, *HuLiS Program: Lewis embedded in Hückel Theory* can be found at <http://www.hulis.free.fr>, **2008**; c) Y. Carissan, D. Hagebaum-Reignier, N. Goudard, S. Humbel, *L'Act. Chim.* **2016**, *406*, 36-40.
- [13] R. S. Begunov, A. A. Sokolov, V. O. Belova, M. E. Solov'ev, *Russ. Chem. Bull.* **2016**, *65*, 644-647.
- [14] K. Fukui, T. Yonezawa, C. Nagata, H. Shingu, *J. Chem. Phys.* **1954**, *22*, 1433-1442.
- [15] Y. Huang, D. Yan, X. Wang, P. Zhou, W. Wu, H. Jiang, *Chem. Commun.* **2018**, *54*, 1742-1745.
- [16] K. M. Saini, R. K. Saunthwal, S. Kumar, A. K. Verma, *J. Org. Chem.* **2019**, *84*, 2689-2698.
- [17] K. Sonogashira, Y. Tohda, N. Hagihara, *Tetrahedron Lett.* **1975**, 4467-4470.
- [18] D. Aburano, T. Yoshida, N. Miyakoshi, C. Mukai, *J. Org. Chem.* **2007**, *72*, 6878-6884.
- [19] N. Mokhtari Brikci-Nigassa, G. Bentabed-Ababsa, W. Erb, F. Chevallier, L. Picot, L. Vitek, A. Fleury, V. Thiéry, M. Souab, T. Robert, S. Ruchaud, S. Bach, T. Roisnel, F. Mongin, *Tetrahedron* **2018**, *74*, 1785-1801.
- [20] C. L. Fleming, P. A. Sandoz, T. Inghardt, B. Oenfelt, M. Grotli, J. Andreasson, *Angew. Chem. Int. Ed.* **2019**, *58*, 15000-15004.
- [21] S. Klaeger, S. Heinzlmeir, M. Wilhelm, H. Polzer, B. Vick, P.-A. Koenig, M. Reinecke, B. Ruprecht, S. Petzoldt, C. Meng, J. Zecha, K. Reiter, H. Qiao, D. Helm, H. Koch, M. Schoof, G. Canevari, E. Casale, S. R. Depaolini, A. Feuchtinger, Z. Wu, T. Schmidt, L. Rueckert, W. Becker, J. Huenges, A.-K. Garz, B.-O. Gohlke, D. P. Zolg, G. Kayser, T. Voeder, R. Preissner, H. Hahne, N. Tonisson, K. Kramer, K. Goetze, F. Bassermann, J. Schlegel, H.-C. Ehrlich, S. Aiche, A. Walch, P. A. Greif, S. Schneider, E. R. Felder, J. Ruland, G. Medard, I. Jeremias, K. Spiekermann, B. Kuster, *Science* **2017**, *358*, 1148.
- [22] a) M. Hedidi, J. Maillard, W. Erb, F. Lassagne, Y. S. Halauko, O. A. Ivashkevich, V. E. Matulis, T. Roisnel, V. Dorcet, M. Hamzé, Z. Fajloun, B. Baratte, S. Ruchaud, S. Bach, G. Bentabed-Ababsa, F. Mongin, *Eur. J. Org. Chem.* **2017**, 5903-5915; b) N. Mokhtari Brikci-Nigassa, L. Nauton, P. Moreau, O. Mongin, R. E. Duval, L. Picot, V. Thiery, M. Souab, B. Baratte, S. Ruchaud, S. Bach, R. Le Guevel, G. Bentabed-Ababsa, W. Erb, T. Roisnel, V. Dorcet, F. Mongin, *Bioorg. Chem.* **2020**, *94*, 103347.
- [23] I. Kazi, S. Guha, G. Sekar, *J. Org. Chem.* **2019**, *84*, 6642-6654.
- [24] L. Wu, X. Liu, C. Z. Ding, S. Chen, L. Hu, L. Zhao, W. Pan, G. Hu, J. Li, *PCT Int. Appl.* 2019, WO 2019015655 A1 20190124.
- [25] S. Ancizu, N. Castrillo, S. Perez-Silanes, I. Aldana, A. Monge, P. Delagrangue, D.-H. Caignard, S. Galiano, *Molecules* **2012**, *17*, 7737-7757.
- [26] X. Liu, C. Qiu, Q. Shen, M. Liu, H. Sheng, G. Du, J. Wang, L. Ding, *PCT Int. Appl.* 2020, WO 2020200191 A1 20201008.
- [27] B. E. Loveland, T. G. Johns, I. R. Mackay, F. Vaillant, Z. X. Wang, P. J. Hertzog, *Biochem. Int.* **1992**, *27*, 501-510.
- [28] N. Ibrahim, P. Bonnet, J.-D. Brion, J.-F. Peyrat, J. Bignon, H. Levaique, B. Josselin, T. Robert, P. Colas, S. Bach, S. Messaoudi, M. Alami, A. Hamze, *Eur. J. Med. Chem.* **2020**, *199*, 112355.

## Entry for the Table of Contents



Oxazolo[5,4-*f*]quinoxalines, thiazolo[5,4-*f*]quinoxalines and pyrazino[*b,e*]isatins were all obtained from 5-iodo-6-aminoquinolines. While the first two families were synthesized by nitrogen functionalization and subsequent copper-catalyzed cyclization, the latter one was obtained by Sonogashira coupling, alkyne hydration and oxidative cyclization. Most of the synthesized polycycles were evaluated in biological tests.

Institute and/or researcher Twitter usernames:

[https://twitter.com/chimie\\_ISCR?ref\\_src=twsrc%5Egoogle%7Ctwcamp%5Eserp%7Ctwgr%5Eauthor](https://twitter.com/chimie_ISCR?ref_src=twsrc%5Egoogle%7Ctwcamp%5Eserp%7Ctwgr%5Eauthor)